

Adsorption kinetics modelling of methylene blue solution by activated carbon using Peleg's equation

N. Bourfis^(1,2*), F. Benaïssa⁽³⁾, S. Benamara⁽¹⁾, H. Gougam⁽¹⁾, K. Louhab⁽¹⁾

¹Food Technology Research Laboratory (LRTA) Faculty of Sciences Engineer
University of M'hamed Bougara, Boumerdes, BP 70, 35000 Boumerdes–Algeria

²University of Akli Mohand Oulhadj Bouira–Algeria.

³Faculty of Sciences, University of M'hamed Bougara, Boumerdes, BP 70, 35000
Boumerdes–Algeria

*Corresponding author: n.bourfis@univ-boumerdes.dz

ARTICLE INFO

Article History:

Received : 17/11/2018

Accepted : 26/06/2019

Key Words:

Activated carbon;

Absorption;

Bitter almond;

Modelling;

Peleg model.

ABSTRACT/RESUME

Abstract: The aim of this study is to envisage the possibility of modelling the adsorption kinetics of methylene blue (MB) by activated carbon using the Peleg's model. Equation often used to describe the sorption and absorption kinetics of water by the material. The study of equilibrium adsorption was also envisaged in this study and the isotherms of Langmuir and Freundlich were tested. The activated carbon was prepared from almond shells bitter, fruit of plants growing in parts of Algeria, especially in the Setif region. Statistical analyses, have proved that the adsorption kinetics of MB by activated carbon is perfectly ($R^2 = 0.9999$) described by the Peleg model. On another hand, the study showed that, compared to the Langmuir model, Freundlich model is most appropriate to describe the equilibrium adsorption.

I. Introduction

Activated carbon is commonly defined as a carbonaceous material showing a well-developed surface area and porous texture [1]. In various forms, this product has been widely used as adsorbent [2] and in catalysis [3, 4] or separation processes [5]. Most of the activated carbons are produced by a two-stages process, carbonization followed by activation. The first step is to enrich the carbon content and to create an initial porosity and the second step is the activation process which helps in enhancing the pore structure [6]. The commonly used precursors to prepare the activated carbon are of different types: bituminous coal, wood, coconut shell, peat, petroleum, pitch, and polymers. Despite its prolific use in adsorption process, the biggest barrier (limiting factor) of its application in the industry is the cost-prohibitive adsorbent and difficulties associated with regeneration [7].

Adsorption is a separation process by which certain components of a fluid phase are attracted to

the surface of a solid adsorbent and form attachments via physical or chemical bonds, thus removing the component from the fluid phase [8]. In general, adsorption processes may be classified as physical or chemical depending on the nature of the involved forces [8]. There are two important physicochemical aspects for the evaluation of adsorption processes as a unit operation: the adsorption equilibrium and the adsorption kinetics [9]. Equilibrium relationships between adsorbent and adsorbate are described by adsorption isotherms, usually by taking into account the ratio between the quantity adsorbed and that remaining in the solution at a fixed temperature at equilibrium. Kinetic study is an important step in the investigation of the adsorption process because it depicts the uptake rate of adsorbate, and controls the residual time of the whole adsorption process [10]. Also, it is important to establish the most appropriate correlation for the isotherms curves in order to optimize the design of an adsorption system [11]. For this reason, several models are used for equilibrium adsorption modelling by

activated carbon. Moreover, the most cited models in the literature are Langmuir [12] and Freundlich [13] equations. Concerning adsorption kinetic, several models are applied: pseudofirst-order [14], pseudo-second order [15], Elovich [16], Diffusion kinetic model [17].

The objective of this study is to investigate the adsorption kinetic modelling by activated carbon from bitter almonds, using the Peleg model [18].

Before, Peleg's model is employed for modelling the phenomenon of water sorption by various foods: corn [19], chickpea [20], orange [21], chicken [22], olive leaves [23]... , it was also used to model dehydration by osmosis [24]. Only one case was reported on the application of Peleg's model outside water exchange and concerns the extraction of soluble matters such as polyphenols [25, 26]. Knowing that this process is a physical phenomenon, it seems it is possible to introduce the Peleg's equation to describe the adsorption kinetics by activated carbon.

The activated carbon used in the present study was prepared from the shells of bitter almonds, fruit of a plant wild which grows in certain regions of north Algeria, especially in Aith- Ouertilène (Setif region). By its considerable proportion in the fruit, the shell is a very valuable linocellulosic material deserving to be evaluated.

II. Material and methods

II.1. Material

The raw material used for the preparation of activated carbon (AC) is the seeds shells of wild bitter almonds (SBAS, hereafter). These are the fruits (Fig.1) of a plant that grows wild in the region of Aith-Ouertilène (Setif region, Algeria). HSBAS analyzed were collected in July 2013.



Figure 1. Some seeds of the analysed wild bitter almonds.

II.2. Preparation of activated carbon

SBAS were washed with distilled water, dried, ground in a laboratory mill and sieved to various particle-size fractions using a conventional sieve shaker. The activation of SBAS was performed according to the procedure followed by Soleimaniet al. (2008) [27] with some minor modifications. SBAS were impregnated with phosphoric acid solution in 1:1 weight ratio. This mixture was left in a drying oven (MEMMERT, Beschickung – Loading Modell 100 - 800) at 100 °C for 24h. The activated material was washed with distilled water

to remove the free acid and the carbon was soaked in 1% NaHCO₃ solution to remove any residual acid [11, 28]. Then, it was washed with distilled water until the pH of the activated carbon reached 6 value. Finally, activated carbon (SBAS carbon) was oven-dried overnight at 100 °C.

II.3. Batch adsorption experiments

The batch adsorption experiments were performed using shaker Jarrest (JLT6-VELP).

II.3.1. Adsorption kinetic study

Kinetic study is important for investigation of an adsorption process because it allows a best comprehension of the whole adsorption [10]. In the present work, 200 ml of MB solution (100 mg/L) was contacted with a given weight of activated carbon in glass bottles. Samples were shaken at ambient temperature (26 °C). During the tests, samples of the slurry were taken at time varied in the range 0–300 min. Then, the carbon was then separated from the liquid. From a curve plotted by the variation of the MB solution concentration (0.0 – 0.1mM), the concentration (C_t , mg/L) of the solution at any time was subsequently analyzed by measuring the absorbance at 665 nm using UV-visible spectrophotometer (Jasco V-530, Japan), and the amount of the adsorbed MB (q_t , mg/g) by the carbon is calculated according to the following equation:

$$q_t = \frac{V(C_0 - C_t)}{W} \quad (1)$$

Where C_0 is the MB concentration (mg/L) at $t = 0$, V is the volume of the solution (L) and W is the mass of the adsorbent (g).

II.3.2. Equilibrium studies

Batch adsorption studies were performed at 22 °C (room temperature) to obtain the equilibrium isotherms. A series of 250 ml glass vessels were employed. Each vessel was filled with 100 ml of methylene blue (MB) solution of various concentrations (0.10; 0.15; 0.20; 0.25 and 0.30 g/L). The equilibrium test study was performed according to the following initial adsorption conditions (preliminary determined by Taguchi designs): pH 2.2 and dried carbon sample of 2 grams per vessel (\emptyset of particles = 0.2-0.63 mm). The solution was mixed at 150 rpm and equilibrated for about 5 h. Subsequently, the carbon particles were separated from the solution by filtration (with Whatman No. 42 filter paper) [27] and clear solutions were analyzed for the MB concentrations by UV-visible spectrophotometer (Jasco V-530, Japan) at a wavelength of 600 nm. The equilibrium concentration (C_e , mg/L) is found experimentally when adsorption reaches its equilibrium state.

The equilibrium concentration (q_e , mg/g) retained in the adsorbent phase was calculated by the following equation:

$$q_e = \frac{V(C_0 - C_e)}{W} \quad (2)$$

II.4. Modelling of adsorption kinetics using Peleg's equation

It is important to establish the most appropriate correlation for the isotherms curves in order to optimize the design of an adsorption system [11].

Peleg [18] proposed the following two parameters sorption equation for prediction accuracy during water vapour adsorption of milk powder and whole rice, and soaking of whole rice:

$$X = X_0 \pm \frac{t}{K_1 + K_2.t} \quad (3)$$

where X_0 and X are the initial moisture content and moisture content at time t expressed as dry basis respectively, K_1 is the Peleg rate constant, and K_2 is the Peleg capacity constant. In (3), “ \pm ” becomes “+” if the process is absorption or adsorption and “-” if the process is drying or desorption.

Peleg rate constant K_1 related to desorption rate at the very beginning ($t = t_0$):

$$\frac{dX}{dt} = \pm \frac{1}{K_{1i}} \quad (4)$$

The Peleg capacity constant K_2 is related to the maximum reached moisture content. As $t \rightarrow \infty$, (5) gives the relation between equilibrium moisture content (X_e) and K_2 :

$$X_e = X_0 \pm \frac{1}{K_2} \quad (5)$$

Linearization of (5) gives:

$$\frac{t}{X - X_0} = K_1 \pm K_2.t_i \quad (6)$$

The plotting of (6) is a straight line, where the first term of the second member is the intercept (K_1) and K_2 is the slope.

II.4.1. Using Peleg's equation in the adsorption phenomena

Similarly, for salt gain the Peleg model can be also written as:

$$\frac{t}{q_t - q_0} = C_1 + C_2.t \quad (7)$$

Where q_t is the MB quantity retained in the adsorbent phase (mg/g) at time t , q_0 is the initial MB quantity and C_1 is the Peleg rate constant, and C_2 is the Peleg capacity constant.

In the phenomenon of adsorption, the quantity (q_0) is null: no quantity of BM adsorbed at t_0 . Equation 7 can then be written:

$$\frac{t}{q_t} = C_1 + C_2.t$$

The Peleg rate constant C_1 is related to q_t at the very beginning, $t = t_0$:

$$\frac{dq_t}{dt} = \frac{1}{C_1} \quad (8)$$

The Peleg capacity constant C_2 is proportional to the maximum reached q_t . As $t \rightarrow \infty$, (9) gives the relation between q_e and C_2 :

$$q_{t,\infty} = q_e = \frac{1}{C_{2i}} \quad (9)$$

Regarding the modelling of adsorption kinetics others models have been used: Pseudo-first-order; Pseudo-second-order; Elovich and Diffusion model.

II.5. Adsorption isotherm

II.5.1. Langmuir equation

The Langmuir adsorption describes the surface as homogeneous assuming that the adsorption sites have equal adsorbate affinity and that adsorption at one site does not affect adsorption at an adjacent site [29]. This model can be described by the following form:

$$\frac{C_e}{q_e} = \frac{1}{Q_0 b} + \frac{C_e}{Q_0} \quad (10)$$

Where q_e is the amount of MB adsorbed at equilibrium (mg/g), C_e is the equilibrium concentration (mg/l), Q_0 is the monolayer adsorption capacity (mg/g) and b is the constant related to the free adsorption energy (Langmuir constant, l/mg). A plot of C_e/q_e versus C_e gives a straight line with the slope $1/Q_0$ which corresponds to complete coverage (mg/g) and the intercept is $1/Q_0 b$.

II.5.2. Freundlich equation

The Freundlich isotherm describes the equilibrium on heterogeneous surfaces and does not assume monolayer capacity [29]. The Freundlich equation is described as follow:

$$\log q_e = \log K_f + \frac{1}{n} \log C_e \quad (11)$$

Where K_f is an indicative constant of the relative adsorption capacity of the adsorbent (mg/g) and the constant $1/n$ indicates the intensity of the adsorption. These constants were calculated from the slope and intercept of the Freundlich plots.

II.6. Data analysis

The fit between the experimental and predicted data was determined using the correlation coefficient (R^2), hybrid fractional error function

(HYBRID), marquart's percentage standard deviation (MPSD), average relative error (ARE)

[11] and the root mean square error (RMSE) [30] as described below:

$$HYBRID = \frac{100}{n-p} \sum_{i=1}^n \left[\frac{(q_{e,exp} - q_{e,cal})^2}{q_{e,exp}} \right] \quad (12)$$

$$MPSD = 100 \sqrt{\frac{1}{n-p} \sum_{i=1}^n \left(\frac{q_{e,exp} - q_{e,cal}}{q_{e,exp}} \right)^2} \quad (13)$$

$$ARE = \frac{100}{n} \sum_{i=1}^n \left| \frac{q_{e,exp} - q_{e,cal}}{q_{e,exp}} \right| \quad (14)$$

$$RMSE = \frac{1}{n} \sqrt{\sum_{i=1}^n (q_{e,exp} - q_{e,calc})^2} \quad (15)$$

Microsoft Excel 2007 was used to perform statistical analysis.

III. Results and discussion

III.1. Modelling of adsorption kinetic

Fig. 2 shows the chart of the BM amount adsorbed by the AC at various time intervals of a liquid phase which is characterized by an initial concentration of 74.7 mg/l. As it can be seen, the carbon adsorption capacity (q_e) increases with time, reaching at the end maximum value of 7.399 mg/g of AC) after a contact time of 100 min approximately. At this time, an equilibrium state, during which ceases any transfer of matter between AC and the liquid medium of immersion, is established.

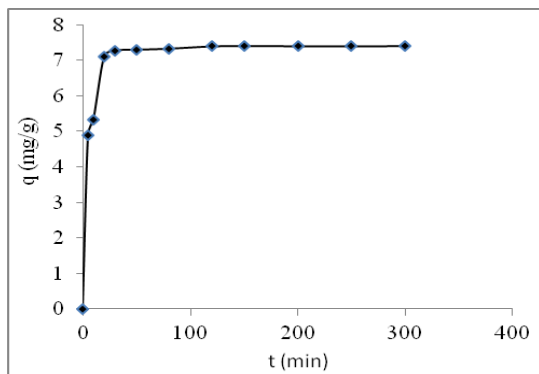


Figure 2. Adsorption kinetics of the MB by AC (at 26 °C).

Really, the curve of adsorption kinetic which is obtained (Fig. 2) takes a similar form to that obtained by Dadali et al. (2008) [31] describing the water uptake kinetic of dried spinaches using Peleg' equation. Obviously, this similarity enables us to envisage the possibility to introduce the Peleg model to investigate the adsorption phenomena.

So, the line airized form (Fig. 3) is applied with the aim of determining the constant characteristics (C_1 and C_2) of the Peleg model.

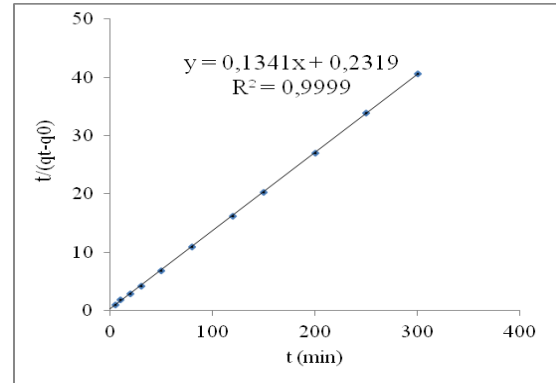


Figure 3. Modeling of the MB adsorption by AC using Peleg's equation.

The found values, together with corresponding statistical parameters, are summarized in Table 1.

Table 1. Values of Peleg's constants (C_1 and C_2) and statistics parameters related to the MB adsorption by AC.

Peleg constants	
C_1 (min.g.mg ⁻¹)	0.232
C_2 (g.mg ⁻¹)	0.134
$q_{e,calc}$ (mg/g)	7.457
Statistics parameters	
R^2	0.9999
HYBRID	3.316
ARE	3.827
RMSE	0.114
MPSD	7.927

The good adequacy of the model tested is supported by the high value of the determination coefficient (R^2), as well as low values of the four other applied statistics. This result is confirmed by the Fig. 4 illustrating experimental results and predicted by the model curves since the two curves stacked almost perfectly.

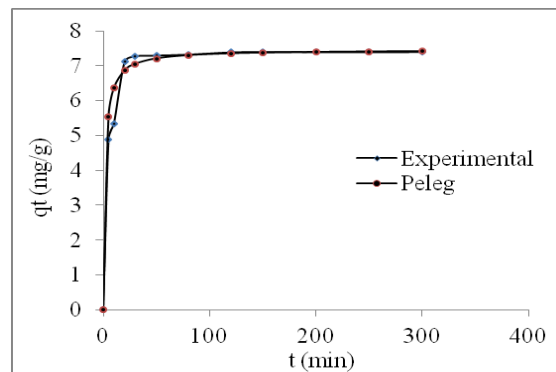


Figure 4. Comparison of experimental and Peleg model curves.

predicted BM adsorption kinetics by AC according to Peleg's model.

This concordance is also established by the good correlation ($R^2 = 0.9717$) between the experimental data (q_{texp}) and those calculated (q_{tcalc}) by the model (Fig.5).

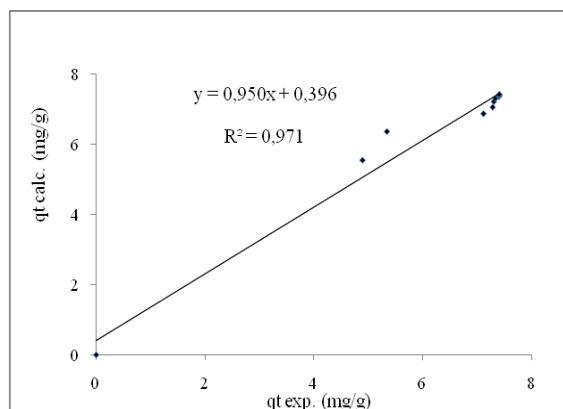


Figure 5. Correlation between the experimentally obtained values of MB adsorbed amount vs. calculated concentrations using Peleg's model.

On the other hand, the adsorption capacity ($q_{e calc} = 7,457$ mg/g) evaluated through (Eq.9) agrees well with that obtained in experiments ($q_{e exp} = 7,399$ mg/g). This is another confirmation of the aptitude Peleg model to describe the BM adsorption process by the activated carbon.

As one had to expect it, the Peleg constants values (C_1 and C_2) obtained in this work are different with those communicated by various authors (Table 2).

These observed differences can be indeed imputed to: 1) the great difference of mechanisms taking place during absorption and adsorption and 2) the nature of the studied material. In all cases, constant C_1 is inversely proportional to the dye fixing what is in concordance with literature data [32].

Table 2. Comparison between Peleg's constants of MB adsorption by AC and those of water absorption.

	C_1 (h.% ⁻¹)	C_2 (% ⁻¹)	T (°C)	R^2	Matter	Reference
MB adsorption	386.67	134260	26	0.9999	-	our study
Water absorption	11900	7400	20	0.990	Pasta	[45]
	17100	7510	30	0.995	Chickpea	[20]
	13.353	3671	25	0.990	cowpea (GC)	[46]
	188.165	3536.7	25	0.990	Bambara groundnuts	[46]
	1.414	16384.723	30	0.9963	Shiitake mushroom	[47]
	240.191	57427.64	20	-	Chilean papaya	[48]
	0.02465	0.00702	20	0.9973	Chickpea (<i>Cicer arietinum</i> L.)	[33]
	0.017225	0.00699	30	0.9928	Chickpea (<i>Cicer arietinum</i> L.)	[33]
Solid-Liquid extraction of total polyphenols	2770	309000	26	0.994	Soybeans	[25]

According to Table 2, the adsorption speed of the dye molecules are greater than that of the water absorption by certain foods, with a factor ranging from 29 (case of Cowpea (GC)) to 22447 (case of chickpeas). As previously underlined, the high observed difference in the C_1 values can be attributed to the difference in the mechanisms staked: the adsorption concerns the interface phenomena, where as the absorption integrates mass transfer into the whole volume of the product.

On the other hand, the adsorption speed (C_1) found in this work is 7 times lower than that of the solid-liquid extraction of total polyphenols from soya [25].

Concerning the constant C_2 , the value is higher than those of the literature. The adsorption capacity found in this work is higher than those related to the water absorption by various foods with a factor ranging from about 2.3 (Chilean Papaya) to 38 (Bambara groundnuts); it is moreover 2.3 times lower than the extraction capacity of the phenolic compounds by ethanol.

It should be noted that the Peleg parameters (C_1 and C_2) are affected by the experimental conditions, more particularly the treatment temperature. Several authors [20, 32, 34, 35, 36]

revealed that these parameters decrease as the temperature increases. The parameter C_2 also depends on the matter nature, the structure of its tissue and its chemical composition [32, 37]. Nevertheless, other authors [35, 38] indicate that C_2 can change if the structure or other properties are affected by the treatment temperature.

IV.2. Adsorption isotherm

The adsorption isotherm shows how the adsorption molecules are distributed between the liquid phase and the solid phase when adsorption reaches equilibrium.

It is well-known that the modelling of adsorptions isotherms is the first objective to be reached in any scientific investigation since it is used as rational mathematical tool for moving from the experimental laboratory to the design of wide prototype.

The variation of the adsorbed dye quantity (q_e) according to the equilibrium concentration (C_e) is shown in Fig. 6.

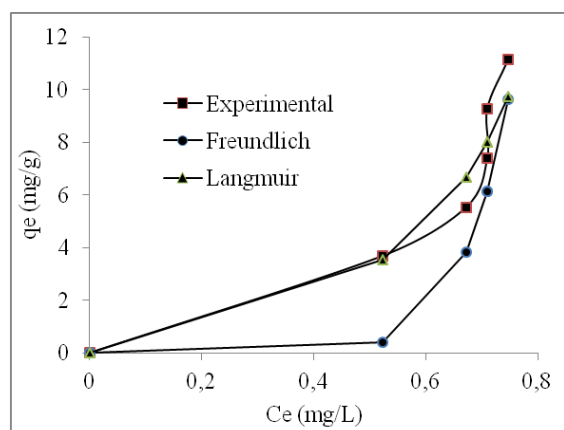


Figure 6. Equilibrium adsorption isotherm of MB by AC (at 26 °C).

It follows that the equilibrium adsorption amount (q_e) increases with the increase of dye concentration (C_e). This finding is consistent with bibliographic data: BM adsorption by bentonite [9], adsorption of the 4-chlorophenol by the activated carbon prepared starting from rattan sawdust [39, 40]), adsorption of copper by the coal of the hazel nut shell [10], adsorption of copper by coal of the almond shell [11], adsorption of the basic dyes (methylene blue, basic 22, yellow red basic 21) by the activated carbon [8], and absorption of the basic dyes (basic blue 3, basic red 22, basic yellow 11) by kudzu [41].

On the other hand, several models are cited in the literature to describe the experimental data related to adsorption isotherms. The Langmuir model and Freundlich model are the most frequently used [40].

The studied Isotherms constants are calculated, each one from the linear equation form of the corresponding model, and are presented in table 3. On this table, the values of the determination coefficient (R^2) like those of the various estimated errors are also shown (HYBRID, ARE and MPSD).

Table 3. Langmuir and Freundlich isotherm constants for MB dye by activated carbon at 26°C.

Constants	Langmuir		Freundlich	
	Q_0 (mg/g)	b (L/mg)	K_f (mg/g)	N
	-3.146	-1.012	124.882	0.114
R^2	0.802		0.898	
HYBRID	21.488		162.317	
ARE	11.861		38.638	
MPSD	16.937		58.837	

From Table 3, the determination coefficient values (R^2), as well as (unfortunately) other statistical characteristics are highest for Freundlich model. At the same time, the negative constants of the Langmuir model imply the inadequacy of this one for the description of the experimental data [42]. Thus it becomes clear that the Freundlich model fit correctly experimental data. It must be recalled that this last, which is of empirical nature, can be employed to describe heterogeneous adsorption, while the Langmuir model suggests that the molecules adsorption is done on a homogeneous surface into full-course without interaction between the adsorbed molecules [40]. However, generally most of authors [8, 10, 11, 39, 40, 43] observed that: 1) equilibrium adsorption isotherm is of type II and that 2) with this type, the Langmuir model is associated. But no theory postulates on automaticity between the type and the model. Moreover, Demirbas et al. (2009) [10] found for the same type II, an almost identical adequacy between the models of Langmuir ($R^2 = 0.999$) and Freundlich ($R^2 = 0.915$). Lastly, our results (concerning the isotherm type and the model type) are in conformity with those communicated by Estevinho et al. (2006) [44] worked on the adsorption of pentachlorophenol by the sweet almond hull in a rough state (without any treatment of neither activation nor carbonization).

This adequacy is proved by the good correlation between $q_{e\text{ exp}}$ and $q_{e\text{ calc}}$ (Fig. 7).

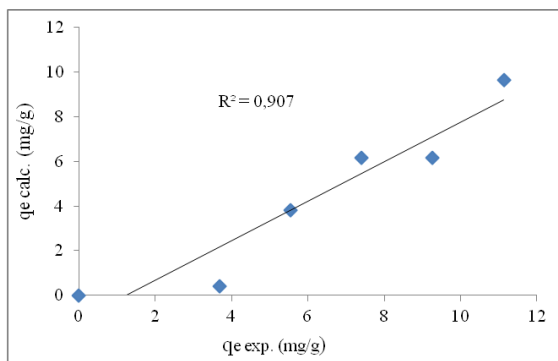


Figure 7. Correlation between the experimentally obtained values of MB adsorbed amount vs. calculated concentrations using Freundlich model.

IV. Conclusion

In this study, the obtained results show clearly that the preparation of an activated carbon from bitter almond shells is possible.

In addition, the adsorption kinetics of the methylene blue is correctly described by Peleg's model. This one, to our knowledge is never introduced earlier for analysis of the adsorption processes.

On other hand, the experimental data reveal that the adsorption capacity of the obtained activated carbon is satisfactory since it is comparable with that of the traditional activated carbon resulting from other types of biomaterials. Moreover, the study proves that, compared with Langmuir model, Freundlich model describes best the adsorption isotherm.

Consequently, the bitter almonds can arouse an interest near the various industrial sectors which will contribute to the safeguard of the biodiversity.

V. References

- Ould-Idriss, A.; Stitou, M.; Cuerda-Correa, E.M.; Fernández-González, C.; Macías-García, A.; Alexandre-Franco, M.F.; Gómez-Serrano, V. Preparation of activated carbons from olive-tree wood revisited. I. Chemical activation with H₃PO₄. *Fuel Processing Technology* 92 (2011) 261–265.
- Rivera-Utrilla, J.; Sanchez-Polo, M.; Gomez-Serrano, V.; Alvarez, P.M.; Alvim-Ferraz, M.C.M.; Dias, J.M. Activated carbon modifications to enhance its water treatment applications. *Journal of hazardous materials* 187 (2011) 1–23.
- Lee, J.; Kim, J.; Hyeon, T. Recent progress in the synthesis of porous carbon materials. *Advanced Materials* 18 (2006) 2073–2094.
- Reimerink, W. M. T. M.; The use of activated carbon as catalyst and catalyst carrier in industrial applications. *Studies in Surface Science and Catalysis A120* (1999) 751–769.
- Dabrowski, A.; Adsorption from theory to practice. *Advances in Colloid and Interface Science* 93 (2001) 135–224.
- Prakash Kumar, B.G.; Shivakamy, K.; Miranda, L. R.; Velan, M. Preparation of steam activated carbon from rubberwood sawdust (*Hevea brasiliensis*) and its adsorption kinetics. *Journal of hazardous materials B136* (2006) 922–929.
- Chen, J.P.; Lin, M. Surface charge and metal ion adsorption on an H-type activated carbon: experimental observation and modelling simulation by the surface complex formation approach. *Carbon* 39 (2001) 1491–1504.
- El Qada, E. N.; Allen, S. J.; Walker, G. M. Adsorption of basic dyes from aqueous solution onto activated carbons. *Chemical Engineering Journal* 135 (2008) 174–184.
- Hong, S.; Wen, C.; He, J.; Gan, F.; Ho, Y.S. Adsorption thermodynamics of methylene blue onto bentonite. *Journal of hazardous materials* 167 (2009) 630–633.
- Demirbas, E.; Dizge, N.; Sulak, M.T.; Kobya, M. Adsorption kinetics and equilibrium of copper from aqueous solutions using hazelnut shell activated carbon. *Chemical Engineering Journal* 148 (2009) 480–487.
- Demirbas, E.; Kobya, M.; Konukman, A.E.S. Error analysis of equilibrium studies for the almond shell activated carbon adsorption of Cr(VI) from aqueous solutions. *Journal of hazardous materials* 154 (2008) 787–794.
- Langmuir, I. Adsorption of gases on plain surfaces of glass mica platinum. *Journal of the American Chemical Society* 40 (1918) 1361–1403.
- Freundlich H.M.F. Über die adsorption in lösungen. *Zeitschrift für Physikalische Chemie* A57 (1906) 385–470.
- Lagergren S. About the theory of so called adsorption of soluble substances. *Ksver Vetenskapsakad Handl* 24 (1898) 1–6.
- McKay, Y. S. Ho, G. Pseudo-second order model for sorption processes. *Process Biochemistry* 34 (1999) 451–465.
- Chien, S. H.; Clayton, W. R. Application of Elovich equation to the kinetics of phosphate release and sorption in soils. *Soil Science Society of America Journal* 44 (1980) 265–268.
- Urano, K.; Tachikawa, H. Process development for removal and recovery of phosphorus from wastewater by a new adsorbent. II. Adsorption rates and breakthrough curves. *Industrial & Engineering Chemistry Research* 30 (1991) 1897–1899.
- Peleg, M. An empirical model for the description of moisture sorption curves. *Journal of Food Science* 53 (1988) 1216–1219.
- Peng, G.; Chen, X.; Jiang, W.; Wu, X. Modeling of water sorption isotherm for corn starch. *Journal of Food Engineering* 80 (2007) 562–567.
- Turhan, M.; Sayar, S.; Gunasekaran, S. Application of Peleg model to study water absorption in chickpea during soaking. *Journal of Food Engineering* 53 (2002) 153–159.
- Díaz, G. R.; Martínez-Monzó, J.; Fito, P.; Chiralt, A. Modelling of dehydration-rehydration of orange slices in combined microwave/air drying. *Innovative Food Science and Emerging Technologies* 4 (2003) 203–209.
- Schmidt, F.C.; Carciofi, B. A. M.; Laurindo, J. B. Application of diffusive and empirical models to hydration, dehydration and salt gain during osmotic treatment of chicken breast cuts. *Journal of Food Engineering* 91 (2009) 553–559.
- Bahloul, N.; Boudhrioua, N.; Kechaou, N. Moisture desorption-adsorption isotherms and isosteric heats of

- sorption of Tunisian olive leaves (*Olea europaea* L.). *Industrial Crops and Products* 28 (2008) 162–176.
24. Corzo, O.; Bracho, N. Application of Peleg model to study mass transfer during osmotic dehydration of sardine sheets. *Journal of Food Engineering* 75 (2006) 535–541.
 25. Jokić, S.; Velić, D.; Bilić, M.; Bučić-kojić, A.; Planinić M.; Tomas S. Modelling of the process of solid-liquid extraction of total polyphenols soybeans. *Czech Journal of Food Sciences* 28 (3) (2010) 206–212.
 26. Boussetta, N.; Lanoisellé, J. L.; Bedel-Cloutour, C.; Vorobiev, E. Extraction of soluble matter from grape pomace by high voltage electrical discharges for polyphenol recovery: Effect of sulphur dioxide and thermal treatments. *Journal of Food Engineering* 95 (2009) 192–198.
 27. Soleimani, M.; Kaghazchi, T. Adsorption of gold ions from industrial wastewater using activated carbon derived from hard shell of apricot stones—An agricultural waste. *Bioresource Technology* 99 (2008) 5374–5383.
 28. Cimino, G.; Cappello, R.M.; Caristi, C.; Toscano, G. Characterization of carbons from olive cake by sorption of wastewater pollutants. *Chemosphere* 61 (2005) 947–955.
 29. Akkaya, G.; Özer, A. Biosorption of Acid Red 274 (AR 274) on *Dicranellavaria*: Determination of equilibrium and kinetic model parameters. *Process Biochemistry* 40 (2005) 3559–3568.
 30. Deng, Y.; Zhao, Y. Effects of pulsed-vacuum and ultrasound on the osmodehydration kinetics and microstructure of apples (Fuji). *Journal of Food Engineering* 85 (2008) 84–93.
 31. Dadali, G.; Demirhan, E.; Özbek, B. Effect of drying conditions on rehydration kinetics of microwave dried spinach. *Food and Bioprocess Technology* 86 (2008) 235–241.
 32. Moreira, R.; Chenlo, F.; Chaguri, L.; Fernandes, C. Water absorption, texture, and color kinetics of air-dried chestnuts during rehydration. *Journal of Food Engineering* 86 (2008) 584–594.
 33. Yildirim, A.; Öner, M. D.; Bayram, M. Modeling of water absorption of ultrasound applied chickpeas (*Cicerarietinum*L.) using Peleg's equation. *Journal of Agricultural Science* 16 (2011) 278–286.
 34. Moreira, R.; Chenlo, F.; Torres, M.D.; Vázquez, G. Effect of stirring in the osmotic dehydration of chestnut using glycerol solutions. *LWT* 40 (2007). 1507–1514.
 35. García-Pascual, P.; Sanjuán, N.; Melis, R.; Mulet, A. *Morchella esculenta* (morel) rehydration process modeling. *Journal of Food Engineering* 72 (2006) 346–353.
 36. Maskan, M. Drying shrinkage and rehydration characteristics of kiwifruits during microwave drying. *Journal of Food Engineering* 48 (2001) 177–182.
 37. Salimi Hizaji, A.; Maghsoudlou, Y.; Jafari, S. M. Application of Peleg model to study effect of water temperature and storage time on rehydration kinetics of air dried potato cubes. *Latin American Applied Research* 40 (2010) 131–136.
 38. Lopez, A.; Pique, M.T.; Clop, M.; Tacias, J.A.; Romero, J. Boatella, J. Garcia, The hygroscopic behaviour of the hazelnut. *Journal of Food Engineering* 25 (1995)197–208.
 39. Hameed, B.H.; Chin, L.H.; Rengaraj, S. Adsorption of 4-chlorophenol onto activated carbon prepared from rattan sawdust. *Desalination* 225 (2008) 185–198.
 40. Hameed, B.H.; Ahmad, A.L.; Latiff, K.N.A. Adsorption of basic dye (methylene blue) onto activated carbon prepared from rattan sawdust. *Dyes and Pigments* 75 (2007) 143–149.
 41. Allen, S.J.; Gan, Q.; Matthews, R.; Johnson, P. A. Kinetic modelling of the adsorption of basic dyes by kudzu. *Journal of Colloid and Interface Science* 286 (2005) 101–109.
 42. Uçar, B.; Güvenç, A.; Ülkü, M. Use of Aluminium hydroxide sludge as adsorbents for the removal of reactive dyes: equilibrium, thermodynamic, and kinetic studies. *Hydrology: Current Research* 2 (2) (2011) 1–8.
 43. Alhamed, Y. A. Adsorption kinetics and performance of packed bed adsorber for phenol removal using activated carbon from dates' stones. *Journal of hazardous materials* 170 (2009) 763–770.
 44. Estevinho, B.N.; Ratola, N.; Alves, A.; Santos, L. Pentachlorophenol removal from aqueous matrices by sorption with almond shell residues. *Journal of hazardous materials* B137 (2006) 1175–1181.
 45. Cunningham, S.E.; McMinn, W.A.M.; Magee, T.R.A.; Richardson, P.S. Modelling water absorption of pasta during soaking. *Journal of Food Engineering* 82 (2007) 600–607.
 46. Kaptso, K.G.; Njintang, Y.N.; Komnek, A.E.; Hounhouigan, J.; Scher, J.; Mbofung, C.M.F. Physical properties and rehydration kinetics of two varieties of cowpea (*Vigna unguiculata*) and bambara groundnuts (*Voandzeia subterranea*) seeds. *Journal of Food Engineering*. 86 (2008) 91–99.
 47. García-Segovia, P.; Andrés-Bello, A.; Martínez-Monzó, J. Rehydration of air-dried Shiitake mushroom (*Lentinus edodes*) caps: Comparison of conventional and vacuum water immersion processes. *LWT - Food Science and Technology* 44 (2011) 480–488.
 48. Zura, L.; Uribe, E.; Lemus-Mondaca, R.; Saavedra-Torrico, J.; Vega-Gálvez, A.; Di Scala, K. Rehydration capacity of Chilean papaya (*Vasconcellea pubescens*): Effect of process temperature on kinetic parameters and functional properties. *Food and Bioprocess Technology* 6 (2013) 844–850.

Please cite this Article as:

Bourfis N., Benaisa F., Benamara S., Gougam H., Louhab K., Adsorption kinetics modelling of methylene blue solution by activated carbon using Peleg's equation, *Algerian J. Env. Sc. Technology*, 6:2 (2020) 1340-1347